AGU PUBLICATIONS

Geophysical Research Letters

RESEARCH LETTER
10.1002/2016GL067795

Key Points:
- C_4N_2 ice clouds in Titan's stratosphere form via solid-state photochemistry
- This alternate ice formation mechanism explains the apparent state of nonequilibrium between C_4N_2 vapor and ice
- Increased dilution in the ice mixture shifts the C_4N_2 ice emission feature to larger wavenumbers

Correspondence to:
C. M. Anderson,
carrie.m.anderson@nasa.gov

Citation:
Anderson, C. M., R. E. Samuelson, Y. L. Yung, and J. L. McLain (2016), Solid-state photochemistry as a formation mechanism for Titan's stratospheric C_4N_2 ice clouds, *Geophys. Res. Lett.*, *43*, 3088–3094, doi:10.1002/2016GL067795.

Received 13 JAN 2016
Accepted 18 MAR 2016
Accepted article online 22 MAR 2016
Published online 14 APR 2016

Solid-state photochemistry as a formation mechanism for Titan's stratospheric C_4N_2 ice clouds

C. M. Anderson[1], R. E. Samuelson[1,2], Y. L. Yung[3], and J. L. McLain[1,2]

[1]NASA Goddard Space Flight Center, Greenbelt, Maryland, USA, [2]Department of Astronomy, University of Maryland, College Park, Maryland, USA, [3]Division of Geological and Planetary Sciences, California Institute of Technology, Pasadena, California, USA

Abstract We propose that C_4N_2 ice clouds observed in Titan's springtime polar stratosphere arise due to solid-state photochemistry occurring within extant ice cloud particles of HCN-HC_3N mixtures. This formation process resembles the halogen-induced ice particle surface chemistry that leads to condensed nitric acid trihydrate (NAT) particles and ozone depletion in Earth's polar stratosphere. As our analysis of the Cassini Composite Infrared Spectrometer 478 cm^{-1} ice emission feature demonstrates, this solid-state photochemistry mechanism eliminates the need for the relatively high C_4N_2 saturation vapor pressures required (even though they are not observed) when the ice is produced through the usual procedure of direct condensation from the vapor.

1. Introduction

Near the winter pole, the cloud structure in Titan's stratosphere is extremely complex compared with that of Earth. The dissimilar stratospheric cloud environments between the two worlds are partly a consequence of Titan's slow rotation, which results in axially symmetric meridional circulation patterns that drive momentum and energy transport in Titan's atmosphere; the outcome is subsidence throughout Titan's winter polar stratosphere. Depending on stratospheric temperature and vapor mole fraction, the condensation of Titan's volatile trace organic vapors onto refractory aerosol particles, hereafter referred to as "aerosols," commences as the volatiles decrease in temperature with the subsiding stratosphere, followed by direct vapor-to-solid phase changes when saturation is achieved. Considering one specific example at 70°N in early northern spring, first benzene (C_6H_6) at 148 km, then cyanoacetylene (HC_3N) at 144 km, and next hydrogen cyanide (HCN) at 136 km in this example, etc., condenses, each time adding a thin shell of ice at a different altitude to the growing ice cloud particle. The order, thickness, and altitude location of each ice shell are strong functions of vapor abundances and temperatures, which vary with latitude and season. By the time the cloud particle arrives at the bottom of the stratosphere near 45 km (tropopause), it has accumulated more than a dozen shells of different volatile organic ices, hereafter referred to as "ices," containing both hydrocarbons and nitriles (see Figure 1) and varying degrees of their mixtures from co-condensation. Co-condensation of HCN and HC_3N begins at 136 km in this example, where HCN first condenses and the HC_3N saturation vapor pressure value has been reduced to one third of its 144 km value. For an overview of the evolution of Titan's condensed ice particles with successive layers, see, e.g., *Sagan and Thompson* [1984], *Frere et al.* [1990], and *Raulin and Owen* [2002].

Dicyanoacetylene (C_4N_2) ice in Titan's stratosphere, however, does not conform to the rule of condensing directly from the vapor once saturation at the ambient temperature is achieved. From the ν_8 C_4N_2 ice emission feature at 478 cm^{-1} observed in Voyager 1 Infrared Interferometer Spectrometer spectra (circa 1980) by *Khanna et al.* [1987] and the corresponding absence of any observed emission from the C_4N_2 vapor phase at 471 cm^{-1}, *Samuelson et al.* [1997] inferred that the upper limit to the C_4N_2 vapor pressure was only ~1% of that required for saturation over the pure ice in Titan's early northern spring polar stratosphere. This result revealed that the C_4N_2 ice and vapor are highly out of vapor-ice equilibrium under the assumption that the ice forms directly from the vapor. Later, *Jolly et al.* [2015] confirmed the absence of the sensitive C_4N_2 vapor emission feature at 107 cm^{-1} in Cassini's Composite InfraRed Spectrometer (CIRS) spectra at early northern spring polar latitudes, acquired roughly one Titan year later, reinforcing the observational result that C_4N_2 vapor has a very low mole fraction in Titan's stratosphere.

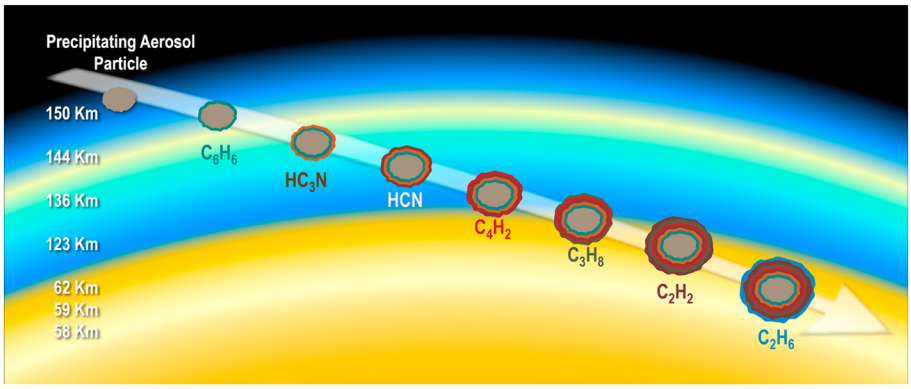

Figure 1. Schematic illustrating ice particle growth via vapor condensation as the particles descend through Titan's stratosphere. Successive ice shells are added each time the particle reaches the level of saturation for a given organic compound. These particles are not perfectly spherical since the initial aerosol nucleus is a fractal aggregate. Not all organic compounds are represented in the schematic. Only vapor condensation processes are considered; solid-state photochemistry is ignored. Image credit: Jay Friedlander.

The principal motivation behind this study is to find an explanation for the extreme deficiency of C_4N_2 vapor in the presence of C_4N_2 ice observed in Titan's early spring polar stratosphere (circa 2010) by Cassini CIRS. Some other mechanism besides that of vapor condensation must be responsible for the observed amount of C_4N_2 ice. We have arrived at a solution involving an alternate mechanism that satisfies both the relatively high C_4N_2 ice abundance and low C_4N_2 vapor pressure while simultaneously maintaining vapor-ice equilibrium. We postulate that C_4N_2 ice is forming via solid-state photochemistry in a volatile condensate mixture of HCN and HC_3N, a process analogous to the heterogeneous surface chemistry on ice particles associated with Earth's polar stratospheric clouds that is ultimately responsible for the Antarctic ozone hole [*Molina et al.*, 1987; *Sander et al.*, 1989].

2. C_4N_2 Vapor-Ice Equilibrium

In order for a stratospheric ice cloud to exist in a steady state (remain time independent), the vapor and ice must be in equilibrium with one another. This requires that the outflux of vapor from the particle surface (evaporation) be numerically equal (though opposite in sign) to the influx at the particle surface (condensation). If C_4N_2 vapor and ice were to depart from equilibrium, the rate at which equilibrium is restored is very rapid. According to *Pruppacher and Klett* [1996], it takes only minutes to reestablish a water vapor partial pressure within 1% of that of saturation if the water ice is formed through direct contact with its vapor. The same should be true for C_4N_2 ice. Since the equilibrium vapor pressure of C_4N_2 in Titan's stratosphere is observed to be much lower (~1%) than that over its pure ice, the formation mechanism of C_4N_2 ice cannot be that of vapor condensation.

In order that Titan's stratospheric C_4N_2 ice clouds remain in a steady state and satisfy vapor-ice equilibrium, the fractional number density of C_4N_2 molecules on an ice particle surface must be only ~1% of that for pure C_4N_2 ice, even though the C_4N_2 fractional number density in the ice particle interior is observed to be much larger. Thus, there is a mole fraction gradient of C_4N_2 between the interior and the surface of a nominal particle containing C_4N_2 ice. A diffusion barrier composed of an ice with a chemical composition other than C_4N_2 is required to maintain this C_4N_2 mole fraction gradient. Without such a barrier, either all of the C_4N_2 ice would quickly evaporate or the C_4N_2 vapor pressure of the ambient atmosphere would rapidly increase to its saturation value over pure C_4N_2 ice at the ambient temperature.

3. Titan's Stratospheric C_4N_2 Ice Chemistry

How does a molecular diffusion ice barrier become established in the outer layers of the particle? Northern winter polar abundances of observed HCN and HC_3N vapors [see, e.g., *Coustenis et al.*, 2007; *Teanby et al.*, 2008; *Vinatier et al.*, 2010], coupled with inferred stratospheric vertical temperature profiles [*Anderson et al.*, 2014, and references therein], suggest that HC_3N vapor condenses at an altitude near 150 km, while HCN vapor condenses just a few kilometers below this altitude [see, e.g., *Anderson et al.*, 2010]. The vapor mole fraction and temperature, which vary with latitude and season, control the altitude at which a given volatile

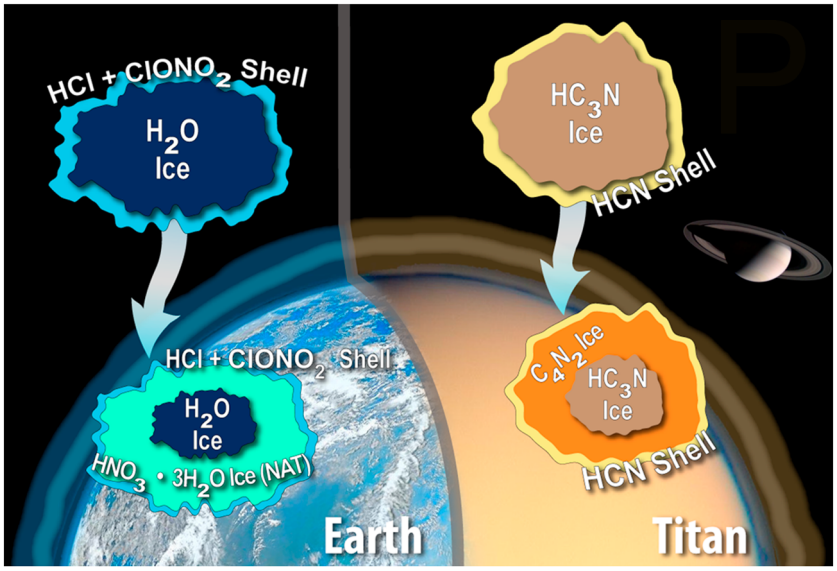

Figure 2. Solid-state chemistry in the stratospheres of Titan and Earth. On Earth, the formation of nitric acid trihydrate [$HNO_3 \cdot 3H_2O$ (NAT)] ice particles is produced via adsorption of HCl and $ClONO_2$ vapors onto preexisting H_2O ice particles. On Titan, dicyanoacetylene (C_4N_2) ice may be produced from adsorption or freezing of HCN vapor onto preexisting cyanoacetylene (HC_3N) ice particles. The production of NAT particles on Earth led to our idea that solid-state chemistry may be occurring in certain stratospheric cloud particles on Titan. Image credit: Jay Friedlander.

will condense. If the ice cloud forms from vapor condensation, which is the case for HCN and HC_3N, the mole fraction of the vapor controls the amount of resulting ice.

Figure 2 illustrates the resulting configuration. HC_3N vapor reaches saturation and condenses onto an aerosol nucleus to form the ice core. The particle then subsides downward a few kilometers to a slightly lower altitude where HCN vapor condenses to form an HCN ice mantle around the precipitating particle. We then postulate that solid-state photochemistry inside the HCN-HC_3N ice particle occurs to produce C_4N_2 ice in the following way:

(R1) $HC_3N + h\nu \longrightarrow H + C_3N$
(R2) $C_3N + HCN \longrightarrow C_4N_2 + H$
(R3) $H + H \longrightarrow H_2$

(R4) net $HCN + HC_3N \longrightarrow C_4N_2 + H_2$

Alternatively, the reactions could proceed as follows:

(R5) $HCN + h\nu \longrightarrow H + CN$
(R6) $CN + HC_3N \longrightarrow C_4N_2 + H$
(R3) $H + H \longrightarrow H_2$

(R4) net $HCN + HC_3N \longrightarrow C_4N_2 + H_2$

According to *Clarke and Ferris* [1996], the fraction of UV radiation reaching Titan's surface at the north pole ranges from ~2% at 165 nm to ~70% at 190 nm. On the other hand, *Cherchneff et al.* [1993] show the photodissociation rate of HC_3N vapor decreases by 2 orders of magnitude over the wavelength range 157–193 nm. This photodissociation rate is about 1 order of magnitude below its peak value, which occurs in the range 130–150 nm. All of this suggests that the photodissociation of HC_3N can occur at the altitude where HC_3N condenses, but quantitative modeling will be required to be definitive. Since the photodissociation rate of HCN vapor tends to peak at shorter wavelengths than that of HC_3N, photolysis of HCN may be less efficient at the HCN condensation levels. The fact that HCN is transparent (nonabsorbing) longward of 200 nm [*Ferris and Guillemin*, 1990] is supportive of reaction (R1) being more probable than reaction (R5). This argues in favor of the production of C_4N_2 taking place near the HC_3N ice core rather than near the surface where HCN

ice is concentrated. This in turn is consistent with a C_4N_2 mole fraction that decreases with increasing radial distance from the particle core.

Reaction (R4) is slightly endothermic by 50 kJ/mol. Any photochemistry initiated in the vapor phase outside of the ice particle will not yield any noticeable buildup of C_4N_2 molecules since the molecules will release the excess energy they acquire through photolysis and decay back into their initial reactants. This may explain the observed deficiency of C_4N_2 vapor in the stratosphere and mesosphere by CIRS and via in situ measurements by Cassini INMS.

On the other hand, ice particles can conduct away excess energy induced by photochemical reactions via molecular and/or lattice vibrations. This stabilizes the formation of C_4N_2 molecules in ice particle interiors, enhancing the production rate of C_4N_2 relative to that in the vapor phase outside the particles; a C_4N_2 mole fraction gradient between a particle's outer surface and inner core is thus established. An outer shell of continuously condensing HCN ice provides the diffusion barrier required to maintain the C_4N_2 mole fraction gradient. In the northern polar winter stratosphere, since HCN vapor is more than an order of magnitude greater than HC_3N vapor, HCN vapor will maintain its inventory long after that of HC_3N, enabling it to preserve the diffusion barrier.

In summary, C_4N_2 ice is produced by solid-state photochemistry and not by vapor condensation. Moreover, a very low C_4N_2 vapor pressure outside the ice particles can be maintained by a diffusion barrier composed of an HCN ice shell, along with the subsequent buildup of additional ice shells with different chemical compositions onto the precipitating ice particles. This leads to a very low C_4N_2 mole fraction at the surface of each ice particle, given the low rate at which C_4N_2 molecules diffuse outward to the particle surface. The net result is to maintain vapor-ice equilibrium in the presence of a very low C_4N_2 vapor-to-ice abundance ratio, about 1.0% or less of the value expected if the vapor were saturated with respect to pure C_4N_2 ice.

A somewhat analogous solid-state chemical process occurs in Earth's winter polar stratosphere (see Figure 2), in which chlorine (Cl) compounds are utilized to produce nitric acid (HNO_3) ice on the surfaces of preexisting water ice cloud particles. Briefly, the terrestrial heterogeneous reaction

(R7) $\quad HCl + ClONO_2 \longrightarrow HNO_3 + Cl_2$

is quite slow in the gas phase but is very fast on the surfaces of water ice particles [*Solomon*, 1999]. The net result is a conversion of reservoir species of chlorine ($HCl + ClONO_2$) to labile Cl_2, followed by the Cl-catalyzed destruction of O_3, which drives the formation of the Antarctic ozone hole [*Molina et al.*, 1987; *Sander et al.*, 1989]. *Toon et al.* [1986] and *Crutzen and Arnold* [1986] proposed that, in addition to H_2O, some of the stratospheric ice particles could include solid nitric acid trihydrate [$HNO_3 \cdot 3H_2O$ (NAT)].

The terrestrial analogy to our proposed process for producing C_4N_2 ice in Titan's stratosphere is not exact. Production of condensed HNO_3 and $HNO_3 \cdot 3H_2O$ in Earth's stratosphere is due to particle surface chemistry. There is no diffusion barrier to restrict the buildup of vaporous HNO_3 and its trihydrate outside the particle. However, unlike Earth, the maintenance of a low C_4N_2 vapor pressure in Titan's ambient atmosphere *does* require such a diffusion barrier that must be in a solid state. Since the mole fraction of HCN vapor is more than an order of magnitude greater than that of HC_3N (this varies with latitude and season), it is actually the abundance of HC_3N that controls the buildup of C_4N_2 ice. Once the limited reservoir of HC_3N ice is exhausted, the production of C_4N_2 ice halts. Excess HCN ice then acts to provide the barrier through which C_4N_2 molecules must diffuse in their migration from the particle interior to the particle surface, where they evaporate and become part of the ambient atmosphere.

Observed relative abundance variations with time of both HC_3N and C_4N_2 ices are qualitatively consistent with the physical and chemical picture presented above. During late northern winter, the 506 cm^{-1} emission feature of HC_3N ice was clearly evident in the CIRS limb-tangent spectra at high northern latitudes, but the 478 cm^{-1} emission feature of C_4N_2 ice was at most very weak at this time [*Anderson et al.*, 2010]. Later, in early spring when Titan's middle and lower stratosphere at high northern latitudes were once again exposed to direct sunlight, the reverse was true; C_4N_2 ice was quite evident, but HC_3N ice was not [*Anderson et al.*, 2014]. This is consistent with a photochemical process in which the photolytic destruction rate of HC_3N ice is roughly equal to the production rate of C_4N_2 ice.

4. Radiative Transfer Modeling

Our physical and chemical picture of C_4N_2 ice production via solid-state photochemistry in Titan's stratosphere can be partially tested with radiative transfer fits to the C_4N_2 ice spectral emission feature at 478 cm^{-1} observed by CIRS in the far IR. Even though pure C_4N_2 ice particles are strongly absorbing in the spectral region around the 478 cm^{-1} emission feature, we expect composite ice C_4N_2 particles to be highly diluted by other ices (notably HCN). Since other ices do not have strong absorptions near 478 cm^{-1}, particles containing substantial amounts of these other ices will yield large-particle-scattering cross sections in this spectral region.

It is therefore necessary to incorporate anisotropic multiple scattering into our radiative transfer formalism. We do not use complex refractive indices $n - ik$ for ice mixtures that are calculated theoretically ab initio; rather, we determine the refractive indices directly from a Kramers-Kronig relationship applied to thin-film transmission spectra of C_4N_2-HCN ice mixtures obtained in our in-house Spectroscopy for Planetary Ices Environments laboratory. We chose to use HCN as the other compound of the mixture besides C_4N_2 because, as indicated near the end of the last section, substantial reserves of HCN ice should be left over from the photochemical production of C_4N_2 ice. The HC_3N ice abundance is much less than that of HCN, and once it is exhausted, the C_4N_2 chemistry will turn off; HCN ice thus contributes both to the chemistry and to the scattering continuum.

Equation (1) below gives the relationship between the C_4N_2 ice mole fraction $q(C_4N_2)$ and the mean radius of a composite C_4N_2 ice particle r_2, where r_1 is the mean radius of a pure C_4N_2 ice particle:

$$q(C_4N_2) = \left[\frac{r_1}{r_2}\right]^3. \quad (1)$$

The equation is valid when the number density of C_4N_2 molecules is independent of particle size.

Mie scattering and absorption ice particle cross sections for lognormal particle size distributions are calculated, along with single-scattering phase functions, for different values of r_2. These single-scattering parameters are then incorporated into a two-stream multiple-scattering plane-parallel approximation adopted from *Hanel et al.* [2003], and results are calculated for an isothermal atmosphere. Sensitivity checks confirm that an isothermal approximation to radiative transfer calculations is adequate in the fitting procedure, principally because contributions to the observed radiation field mostly originate in the region immediately surrounding the minimum limb-tangent altitude. The wavelength dependence for aerosol volume absorption coefficients was adopted from *Anderson and Samuelson* [2011].

5. Results and Discussion

An observed CIRS spectrum at 70°N latitude acquired in early northern spring (circa 2010) is shown in Figure 3 and consists of an average of three groups of CIRS limb-tangent spectra, each group containing 84 individual spectra. The average limb-tangent altitude of the center of the field of view (FOV) is 150 km, so only the stratospheric particulates (ices and aerosol) contribute significantly to the spectral continuum.

Radiative transfer fits to the CIRS limb average spectrum are shown in Figure 3 for three $q(C_4N_2)$ values: 1.0 in Figure 3a, 0.5 in Figure 3b, and 0.2 in Figure 3c. We adopt a mean particle radius r_1 of 2.3 μm for HC_3N ice particles at 70°N that was derived by *Anderson et al.* [2010]. We then make the speculative assumption that, in the presence of sunlight (season is early northern spring), all the HC_3N ice is converted to C_4N_2 ice through reaction (R4). We then use the three C_4N_2 mole fractions listed above to calculate mean particle radii r_2 from equation (1). These C_4N_2 mole fractions correspond to r_2 values of 2.3, 2.9, and 3.9 μm. These mean radii are incorporated into the Mie scattering calculations.

Because of the simplistic approximations we made regarding both multiple scattering and the temperature structure, absolute determinations of C_4N_2 ice abundances are rather uncertain and are therefore not given here. However, the calculated spectral shape of the 478 cm^{-1} C_4N_2 ice feature should be fairly accurate. In particular, the fit for both the position and width of the 478 cm^{-1} emission feature of C_4N_2 ice is quite good for $q(C_4N_2) = 0.2$, considering the noisy nature of the observed spectrum. This result suggests that C_4N_2 ice particles are highly diluted, consistent with the need for effective molecular diffusion barriers in each particle. The resulting shift of the C_4N_2 ice emission feature to higher wavenumbers for the more dilute ices is in part due to the real part of the refractive index correspondingly becoming more symmetrical about the central

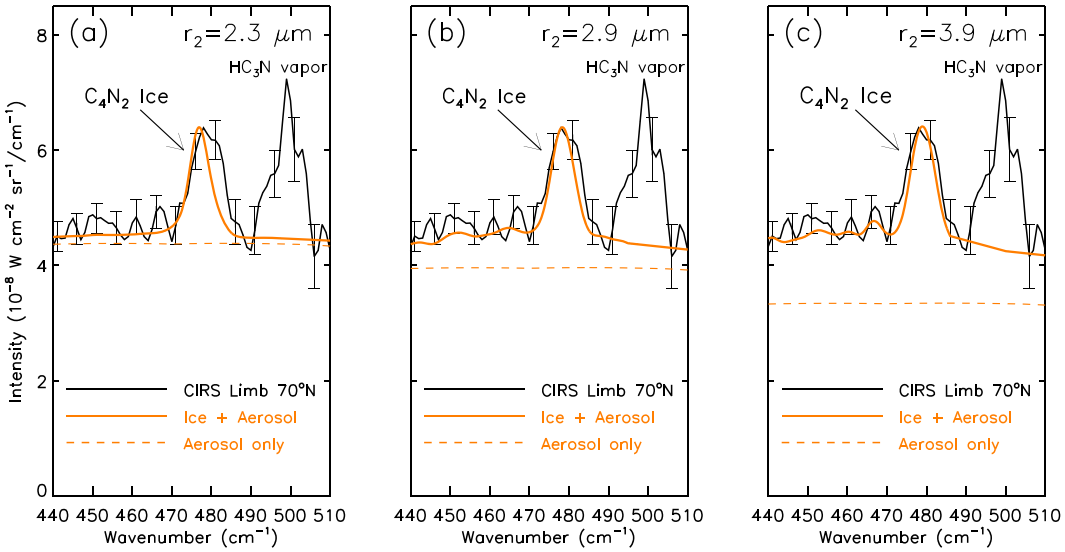

Figure 3. Radiative transfer fits (solid orange curves) to the continuum of CIRS limb-tangent spectral averages at 70°N (solid black curve). The spectral range is limited to 440–510 cm^{-1}, and the C_4N_2 ice feature at 478 cm^{-1} is included in the fits. A simplified two-stream plane-parallel model, patterned after the one by *Hanel et al.* [2003], is used to include effects due to anisotropic multiple scattering. Single-scattering parameters are calculated for various C_4N_2-HCN abundance ratios and mean particle radii: (a) pure C_4N_2 ice, r_2 = 2.3 μm; (b) 50:50 C_4N_2-HCN ice mixture, r_2 = 2.9 μm; and (c) 20:80 C_4N_2-HCN ice mixture, r_2 = 3.9 μm. Orange dashed curves show aerosol contributions. The 1σ error bars are spaced every 5 cm^{-1}.

emission frequency near 478 cm^{-1} and due in part to a shift to higher wavenumbers of the imaginary part of the refractive index.

We also note that both aerosol and ice contribute substantially to the continuum intensity for $q(C_4N_2) = 0.2$. The aerosol is the dominant source of emitted radiation in the continuum, while the ice is responsible for the redistribution of this radiation by scattering.

The results of this study are highly preliminary and serve only to introduce likely chemical and physical processes leading to the production of C_4N_2 ice in Titan's lower stratosphere. We postulate that solid-state photochemistry in the interior of an HCN-HC_3N composite ice particle, rather than the direct condensation of C_4N_2 vapor onto the surface of the particle, leads to the presence of C_4N_2 ice in Titan's lower stratospheric cloud system near the early spring pole. A protective shell of another ice (e.g., HCN) provides a barrier through which molecules of C_4N_2 can leak only slowly, enabling C_4N_2 vapor-ice equilibrium to prevail for remarkably small C_4N_2 vapor partial pressures (~1% saturation vapor pressure over the pure ice).

However, many details need to be investigated more quantitatively before the validity of our process can be fully assessed. For example, What are the rates of C_4N_2 ice formation in the interiors of particles composed of HCN-HC_3N ice mixtures? How does this compare with the rate of C_4N_2 vapor buildup (or breakdown) through photolysis? What are the rates of diffusion through an HCN ice barrier for C_4N_2 molecules and CN and C_3N radicals, and what C_4N_2 mole fraction gradient results?

Although quantitative investigations of these and other questions lie outside the scope of the present study, a few advances are already under way. The photochemical model of Titan developed by *Yung et al.* [1984] has recently been updated in light of Cassini Ultraviolet Imaging Spectrograph and CIRS measurements [*Liang et al.*, 2007; *Li et al.*, 2014, 2015]. Reactions (R1)–(R6) have been incorporated into the model, and preliminary microphysical modeling using the Community Aerosol and Radiative Model for Atmospheres [*Bardeen et al.*, 2010] provides a highly provisional initial estimate that the equivalent of a vertical column of 1×10^{17} molecules cm^{-2} of C_4N_2 may be sequestered in Titan's atmospheric particles. We are also in the process of replacing our simple plane-parallel two-stream radiative transfer scattering model with the spherical-shell model of *Mayo and Samuelson* [2005], which also incorporates a realistic atmospheric thermal structure. In addition, we are also replacing Mie particle-scattering theory with one involving particles with multiple shells. These improvements will allow a more rigorous determination of C_4N_2 ice abundance from

fits to the CIRS 478 cm^{-1} emission feature. If, after further investigations (both theoretical and laboratory), it is demonstrated that our solid-state photochemical model for the production of C_4N_2 ice proves reliable, it opens the door to investigating the production of other volatile ices in the atmospheres of Titan and the major planets without the need for vapor condensation.

Acknowledgments
The authors acknowledge funding support from NASA's Cassini Project. C.M.A. and R.E.S. were supported in part by the Cassini Data Analysis and Participating Scientist program. Y.L.Y. was supported in part by the Cassini UVIS program via NASA grant JPL.1459109 to the California Institute of Technology. The CIRS data presented here are archived in the PDS Atmospheres Node at New Mexico State University.

References

Anderson, C. M., and R. E. Samuelson (2011), Titan's aerosol and stratospheric ice opacities between 18 and 500 μm: Vertical and spectral characteristics from Cassini CIRS, *Icarus*, *212*, 762–778.
Anderson, C. M., R. E. Samuelson, G. L. Bjoraker, and R. K. Achterberg (2010), Particle size and abundance of HC_3N ice in Titan's lower stratosphere at high northern latitudes, *Icarus*, *207*, 914–922.
Anderson, C. M., R. E. Samuelson, R. K. Achterberg, J. W. Barnes, and F. M. Flasar (2014), Subsidence-induced methane clouds in Titan's winter polar stratosphere and upper troposphere, *Icarus*, *243*, 129–138.
Bardeen, C. G., O. B. Toon, E. J. Jensen, D. R. Marsh, and V. L. Harvey (2008), Numerical simulations of the three-dimensional distribution of meteoric dust in the mesosphere and upper stratosphere, *J. Geophys. Res.*, *113*, D17202, doi:10.1029/2007JD009515.
Bardeen, C. G., O. B. Toon, E. J. Jensen, M. E. Hervig, C. E. Randall, S. Benze, D. R. Marsh, and A. Merkel (2010), Numerical simulations of the three-dimensional distribution of polar mesospheric clouds and comparisons with Cloud Imaging and Particle Size (CIPS) experiment and the Solar Occultation For Ice Experiment (SOFIE) observations, *J. Geophys. Res.*, *115*, D10204, doi:10.1029/2009JD012451.
Cherchneff, I., A. E. Glassgold, and G. A. Mamon (1993), The formation of cyanopolyyne molecules in IRC + 10216, *Astrophys. J.*, *410*, 188–201.
Clarke, D. W., and J. P. Ferris (1996), Mechanism of cyanoacetylene photochemistry at 185 and 254 nm, *J. Geophys. Res.*, *101*, 7575–7584.
Coustenis, A., et al. (2007), The composition of Titan's stratosphere from Cassini/CIRS mid-infrared spectra, *Icarus*, *189*, 35–62.
Crutzen, P. J., and F. Arnold (1986), Nitric acid cloud formation in the cold antarctic stratosphere—A major cause for the springtime 'ozone hole', *Nature*, *324*, 651–655.
Ferris, J. P., and J. C. Guillemin (1990), Photochemical cycloaddition reactions of cyanoacetylene and dicyanoacetylene, *J. Org. Chem.*, *55*(21), 5601–5606.
Frere, C., F. Raulin, G. Israel, and M. Cabane (1990), Microphysical modeling of Titan's aerosols—Application to the in situ analysis, *Adv. Space Res.*, *10*, 159–163.
Hanel, R. A., B. J. Conrath, D. E. Jennings, and R. E. Samuelson (2003), *Exploration of the Solar System by Infrared Remote Sensing: Second Edition*, Cambridge Univ. Press, Cambridge, New York, Port Chester, Melbourne, and Sydney.
Jolly, A., V. Cottini, A. Fayt, L. Manceron, F. Kwabia-Tchana, Y. Benilan, J.-C. Guillemin, C. Nixon, and P. Irwin (2015), Gas phase dicyanoacetylene (C_4N_2) on Titan: New experimental and theoretical spectroscopy results applied to Cassini CIRS data, *Icarus*, *248*, 340–346.
Khanna, R. K., M. A. Perera-Jarmer, and M. J. Ospina (1987), Vibrational infrared and raman spectra of dicyanoacetylene, *Spectrochim. Acta Part A*, *43*, 421–425.
Li, C., X. Zhang, J. A. Kammer, M.-C. Liang, R.-L. Shia, and Y. L. Yung (2014), A non-monotonic eddy diffusivity profile of Titan's atmosphere revealed by Cassini observations, *Planet. Space Sci.*, *104*, 48–58.
Li, C., X. Zhang, P. Gao, and Y. Yung (2015), Vertical distribution of C_3-hydrocarbons in the stratosphere of Titan, *Astrophys. J. Lett.*, *803*, L19.
Liang, M.-C., Y. L. Yung, and D. E. Shemansky (2007), Photolytically generated aerosols in the mesosphere and thermosphere of Titan, *Astrophys. J. Lett.*, *661*, L199–L202.
Mayo, L. A., and R. E. Samuelson (2005), Condensate clouds in Titan's north polar stratosphere, *Icarus*, *176*, 316–330.
Molina, M. J., T.-L. Tso, L. T. Molina, and F. C.-Y. Wang (1987), Antarctic stratospheric chemistry of chlorine nitrate, hydrogen chloride, and ice: Release of active chlorine, *Science*, *238*, 1253–1257.
Pruppacher, H., and J. Klett (1996), *Microphysics of Clouds and Precipitation*, Atmospheric and Oceanographic Sciences Library, Springer, Netherlands.
Raulin, F., and T. Owen (2002), Organic chemistry and exobiology on Titan, *Space Sci. Rev.*, *104*, 377–394.
Sagan, C., and W. R. Thompson (1984), Production and condensation of organic gases in the atmosphere of Titan, *Icarus*, *59*, 133–161.
Samuelson, R. E., L. A. Mayo, M. A. Knuckles, and R. J. Khanna (1997), C_4N_2 ice in Titan's north polar stratosphere, *Planet. Space Sci.*, *45*, 941–948.
Sander, S. P., R. R. Friedl, and Y. L. Yung (1989), Rate of formation of the ClO dimer in the polar stratosphere—Implications for ozone loss, *Science*, *245*, 1095–1098.
Solomon, S. (1999), Stratospheric ozone depletion: A review of concepts and history, *Rev. Geophys.*, *37*, 275–316.
Teanby, N. A., et al. (2008), Global and temporal variations in hydrocarbons and nitriles in Titan's stratosphere for northern winter observed by Cassini/CIRS, *Icarus*, *193*, 595–611.
Toon, O. B., J. Pinto, P. Hamill, and R. P. Turco (1986), Condensation of HNO_3 and HCl in the winter polar stratospheres, *Geophys. Res. Lett.*, *13*, 1284–1287.
Vinatier, S., et al. (2010), Analysis of Cassini/CIRS limb spectra of Titan acquired during the nominal mission I. Hydrocarbons, nitriles and CO_2 vertical mixing ratio profiles, *Icarus*, *205*, 559–570.
Yung, Y. L., M. Allen, and J. P. Pinto (1984), Photochemistry of the atmosphere of Titan—Comparison between model and observations, *Astrophys. J. Suppl.*, *55*, 465–506.